Zic1 Promotes the Expansion of Dorsal Neural Progenitors in Spinal Cord by Inhibiting Neuronal Differentiation

Jun Aruga,[*,1] **Takahide Tohmonda,**[*,‡] **Shunsaku Homma,**[†] **and Katsuhiko Mikoshiba**[*,‡]

Laboratory for Developmental Neurobiology, RIKEN Brain Science Institute, Wako-shi, Saitama 351-0198, Japan; †Department of Anatomy, Fukushima Medical University, Fukushima-shi, Fukushima 960-1295, Japan; and ‡Division of Molecular Neurobiology, Department of Basic Medical Science, Institute of Medical Science, University Tokyo, Minato-ku, Tokyo 108-8639, Japan

The role of *Zic1* was investigated by altering its expression status in developing spinal cords. *Zic* genes encode zinc finger proteins homologous to *Drosophila* Odd-paired. In vertebrate neural development, they are generally expressed in the dorsal neural tube. Chick *Zic1* was initially expressed evenly along the dorsoventral axis and its expression became increasingly restricted dorsally during the course of neurulation. The dorsal expression of *Zic1* was regulated by Sonic hedgehog, BMP4, and BMP7, as revealed by their overexpressions in the spinal cord. When *Zic1* was misexpressed on the ventral side of the chick spinal cord, neuronal differentiation was inhibited irrespective of the dorsoventral position. In addition, dorsoventral properties were not grossly affected as revealed by molecular markers. Concordantly, when *Zic1* was overexpressed in the dorsal spinal cord in transgenic mice, we observed hypercellularity in the dorsal spinal cord. The transgene-expressing cells were increased in comparison to those of truncated mutant *Zic1*-bearing mice. Conversely, we observed a significant cell number reduction without loss of dorsal properties in the dorsal spinal cords of *Zic1*-deficient mice. Taken together, these findings suggest that *Zic1* controls the expansion of neuronal precursors by inhibiting the progression of neuronal differentiation. Notch-mediated inhibition of neuronal differention is likely to act downstream of *Zic* genes since *Notch1* is upregulated in *Zic1*-overexpressing spinal cords in both the mouse and the chick.   © 2002 Elsevier Science (USA)

Key Words: Zic; transcription factor; neural development; neuronal differentiation; neuronal progenitors; spinal cord; dorsoventral patterning; Notch signaling; Sonic hedgehog; bone morphogenetic protein.

INTRODUCTION

Zic genes encode zinc finger proteins, which were found to be expressed in the adult mouse cerebellum in a highly restricted manner (Aruga *et al.,* 1994, 1996). These genes are vertebrate homologues of the *Drosophila* pair-rule gene *odd-paired* (Benedyk *et al.,* 1994; Aruga *et al.,* 1996). All members of the *Zic* family share highly conserved zinc finger domains, which are also similar to those of Gli-Ci zinc finger proteins (Ruppert *et al.,* 1988; Hui *et al.,* 1995). To date, several *Xenopus* and mouse genes have been reported. In developing animals, *Zic* gene expressions can

be detected at gastrulation in the ectoderm and mesoderm (Nagai *et al.,* 1997; Nakata *et al.,* 1997, 1998). During organogenesis, their expressions are restricted to the dorsal neural tube, somites, and limb buds. At the adult stage, all mouse *Zic* genes are strongly expressed in the cerebellum. The expression patterns of *Zic* genes are similar to, but distinct from, each other.

Functional analyses of *Xenopus* embryos indicated that they are involved in the initial phase of both neural and neural crest development (Nakata *et al.,* 1997, 1998; Brewster *et al.,* 1998; Kuo *et al.,* 1998; Mizuseki *et al.,* 1998). Furthermore, disruption of the mouse *Zic1* gene leads to hypoplasia and abnormal foliation of the cerebella (Aruga *et al.,* 1998), which occurs at later stages of neural development. These findings indicate that *Zic* genes play critical

roles in the early and later phases of neural development. However, the role of the *Zic* gene in the intervening stage has not yet been elucidated. In particular, the roles of *Zic* genes in the dorsal spinal cord, where all members are expressed in an overlapping fashion, are not well understood.

Accumulated evidence indicates that key molecules exist in the dorsoventral specification of the spinal cord. Sonic hedgehog (Shh), a protein secreted by the notochord and the floor plate, promotes the generation of motor neurons (Echelard *et al.,* 1993; Roelink *et al.,* 1995). This is a ventral property of the neural tube. On the other hand, secretory factors belonging to the TGFβ superfamily, such as BMP4, BMP7, and GDF, are involved in generating dorsally located interneurons (Dickinson *et al.,* 1995; Liem *et al.,* 1995, 1997; Lee *et al.,* 1998). In addition to these secretory factors, several transcription factors are known to be expressed in a restricted manner along the dorsoventral axis. For example, *Pax* genes are expressed in a broad domain and LIM homeodomain genes are expressed in the differentiated neuronal population of the spinal cord (Stuart *et al.,* 1994; Sánchez-Garcia and Rabbitts, 1994).

To clarify the role of *Zic* genes in vertebrate spinal cord development, we studied the role of *Zic1* in chick and mouse developing spinal cords. First, we identified and misexpressed chick *Zic1* (*CZic1*) by *in ovo* electroporation. Then, the spinal cord phenotypes of the *Zic1*-overexpressing and *Zic1*-deficient mice were analyzed. The results indicate that *Zic1* inhibits neuronal differentiation by activating Notch signaling, thereby expanding dorsal neural progenitors.

MATERIALS AND METHODS

Animals

White leghorn chicken embryos were incubated at 37.6°C in a humidified incubator. Stages were determined according to Hamburger and Hamilton (1951). *Zic1*-deficient mice were produced and maintained as previously described (Aruga *et al.,* 1998). In this study, we used mice that had been back-crossed with C57BL/6 five times. The embryonic day (E)0.5 was defined as noon of the day when a vaginal plug was observed. The mice were maintained by the Advanced Technology Development Center, RIKEN Brain Science Institute. All animal experiments were carried out according to the guidelines for animal experimentation in RIKEN.

cDNA Cloning and Plasmid Construction

RNA was isolated from the chick embryo as previously described (Aruga *et al.,* 1994). A chick embryo cDNA library (stage 16–20) was made by using the ZAP Express vector (Stratagene) according to the manufacturer's instruction. The library and a chick embryo forebrain cDNA library provided by Dr. H. Fujisawa were screened. *CZic* cDNA probes were generated by PCR using a pair of primers, 5′-GA-GAACCTCAAGATCCACAA-3′ and 5′-GACTCATGGACCTTC-ATGTG-3′, which were based on the conserved sequence between the mouse *Zic* genes (Aruga *et al.,* 1996). The resulting 210-bp PCR

fragments were used for cDNA library screening. The chick Shh was cloned from the same libraries by using probes generated by PCR. The screening and sequencing were performed as described previously (Aruga *et al.,* 1994).

The MTZic1 expression vector was constructed as follows. A DNA fragment containing the *CZic1* open reading frame was obtained by PCR amplification with the *CZic1* cDNA template. The amplified fragment was inserted into the pCS2 + MT (Turner and Weintraub, 1994) vector, which carries an epitope tag derived from c-myc protein at the 5′ end of the insert (MTZic1). Subsequently, the Myc epitope-tagged *CZic1* fragment was cloned into a pEF-BOS vector, which drives gene expression under the control of the human EF-1α promoter (Mizushima and Nagata, 1990). The chick *Shh,* mouse *BMP4* (supplied by Dr. K. Shibuya), and mouse *BMP7* cDNA (supplied by Dr. R. Beddington) were inserted into pEF-BOS to express these DNAs by electroporation.

In Situ Hybridization

In situ hybridization on sections or whole-mount specimens was performed as previously described (Nakata *et al.,* 1998). Briefly, embryos were fixed in 4% paraformaldehyde in 0.1 M sodium phosphate buffer (pH 7.4) for 12 h. Hybridization was carried out overnight at 60°C in a hybridization mixture (50% formamide, $5\times$ SSPE, 5% SDS, 1 μg/ml yeast transfer RNA) with a denatured RNA probe. DIG-labeled molecules were detected by using NBT/BCIP (Boehringer) as a substrate for the anti-DIG-antibody coupled alkaline phosphatase. *In situ* hybridization for notochord-transplanted embryos was carried out using a ^{35}S-labeled probe, as described (Aruga *et al.,* 1994). Templates for chick Notch1 (AF159231), chick Delta1 (U26590), mouse Notch1 (NM_008714), and mouse HES1 (D16464) probes were generated by PCR. Primer sequences will be supplied on request.

Antibodies and Immunohistochemistry

A rabbit polyclonal antibody against the carboxy-terminal portion of the mouse Zic1 protein (Aruga *et al.,* 1994) was used to detect the chick Zic proteins. This antibody recognizes chick Zic1 as well as chick Zic3, which is expressed in the developing spinal cord in a similar manner to Zic1 (J.A. and T.T., unpublished observations). Antibodies against Lim1/2 (4F2), Islet1 (39.4D5), Msx1/2 (4G1), Pax6, and Pax7 (Monaghan *et al.,* 1991; Sánchez-Garcia *et al.,* 1994; Stuart *et al.,* 1994) were obtained from the Developmental Studies Hybridoma Bank. Anti-Math1 antibody (Helms and Johnson, 1998) was supplied by Dr. J. Johnson. Anti-βIII tubulin (Promega), anti-Myc epitope (9E10, Santa-Cruz), and anti-β-galactosidase (Cappel) antibodies were purchased. The tissues were fixed with 4% paraformaldehyde/0.1 M sodium phosphate buffer (pH 7.4). The fixed embryos were immersed in 20% sucrose overnight, embedded in OCT compound, and sectioned at 12 μm. The primary antibodies were detected with anti-mouse or rabbit IgG conjugated to FITC, TRITC, or Cy3 (Jackson ImmunoResearch) for immunofluorescence staining. For anti-β-galactosidase staining, the embryos were immersed in Bouin's fixative, embedded in paraffin, and sectioned at 6 μm, and the primary antibody was detected with Vectastain ABC kit (Vector Laboratories) and 3,3′-diaminobenzidine as a chromogenic substrate.

Transplantation and in Ovo Electroporation

Notochord transplantation was performed as described (Yamada *et al.,* 1991). The *in ovo* electroporation was performed as described

(Sakamoto *et al.,* 1998; Funahashi *et al.,* 1999 in detail). Briefly, the vitelline membrane covering the caudal part of the stage 10 spinal cord was removed. DNA solution (5 mg/ml in Tris-EDTA buffer) containing Fast Green (200 nl) was injected into the closing posterior neuropore. The electrode (0.5 mm in diameter, 1.0 mm in length, 4 mm between electrodes) was placed on the vitelline membrane. Then, a 30-V, 50-ms rectangular pulse was applied five times by means of a CUY 21 (Tokiwa Science, Fukuoka) electroporator.

In most experiments, a green fluorescence protein expression vector (pEGFP-N1; Clontech) was included in the plasmid solution at a concentration of 0.5 mg/ml for monitoring the state of transfection. As a control for the misexpression experiments, an empty expression vector, pEF-BOS was electroporated under the same conditions. Small spinal cord anomalies were observed after the control transfection. Overexpression was confirmed immunohistochemically by using anti-myc antibody (9E10) for epitope-tagged chick Zic1 protein (MTZic1) and antibodies against Zic1 and SHHN for mouse Zic1 and chick Shh, respectively. Coexpression of MTZic1 and GFP was observed in more than 90% of the cells under the current conditions as in an earlier study (Dubreuil *et al.,* 2000). The validity of the BMP4 and BMP7 expression vector was verified by a biological response which was observed in an overexpression experiment in the osteogenic cell lines (data not shown).

Generation of Zic1-Overexpressing Transgenic Mouse

A *Bam*HI 9-kb fragment of the mouse *Zic1* gene (Aruga *et al.,* 1996, 2000) was used for transgene construction. Initially, the fragment was subcloned into a Bluescript vector (Stratagene), which was modified to have *Not*I sites at both ends of the 9-kb fragment. For both *Z19K* and *TR9K* transgenes, an internal ribosomal entry site (ires) (Jang *et al.,* 1989)-LacZ cassette was inserted into a *Xho*I site located in the 3′ untranslated region. To produce the *TR9K* transgene, a termination-*Sac*I linker (5′-TGAGCTCA-3′) was inserted at the *Hpa*I site of *Z19K,* which was located just 475 bp downstream of the initiation codon, before the LacZ cassette insertion. The plasmids were digested with *Not*I and the vector sequence was removed before microinjection.

The transgenic mice were produced at NihonSLC (Shizuoka, Japan) by microinjecting the transgene DNA into the male pronuclei of fertilized eggs obtained from C57BL/6 × DBA2 F1 female mice. In this study, we used mice that had been back-crossed twice with C57BL/6J. Transgene incorporation was assayed by PCR, as described previously (Aruga *et al.,* 2000).

Cell Death Assay

Cell death was assessed by TUNEL (Terminal deoxynucleotidyl transferase-mediated dUTP-X nick-end labeling) staining and immunohistochemical staining using anti-single strand DNA antibody (DAKO). The TUNEL staining was performed according to the manufacturer's instructions (*In situ* cell death detection kit, POD; Boehringer Mannheim).

Histology and Morphometric Analyses

Hematoxylin and eosin staining and morphometric analyses were performed as described (Aruga *et al.,* 1998). For the quantitative analyses, four independent litters were used to measure spinal cord areas. All histological inspections of the mouse spinal cord were carried out at the tracheal bifurcation level after serial sectioning of entire thoracic spinal cords.

RESULTS

Expression of Chick Zic1 in the Developing Spinal Cord

To begin with, we cloned *CZic1* cDNA from chick embryo libraries. *CZic1* expression was first examined by *in situ* hybridization. *CZic1* transcript was detected before stage 8 (unpublished observation). The expression patterns in the earlier stages will be described elsewhere. During neurulation, *CZic1* expression was detected in the dorsal neural fold, neural tube, and dorsomedial somites (Figs. 1A and 1B). This expression was detected in the entire neural tube along the anterior to posterior axis. Expressions in the neural tube and somites continued thereafter (Figs. 1C–1F, stages 17 and 23). Expressions in the somites and their derivatives were limited to dorsal sclerotomes, and dorsal dermomyotomes including the dorsal lips. As a consequence, *CZic1* was expressed in the neural tissue and paraxial mesoderm and their derivatives. The expression profile is analogous to that of mouse *Zic1* (Aruga *et al.,* 1994; Nagai *et al.,* 1997).

We next examined the localization of chick Zic proteins in the developing spinal cord. Up to stage 8 (Figs. 2A and 2B), chick Zic proteins were distributed evenly along the dorsoventral axis. At stage 9, the ventral staining weakens (Figs. 2C and 2D). Approximately one-fourth of dorsal neural cells were demarcated by immunostaining at stage 17 (Figs. 2E and 2F). However, the staining in the most lateral (dorsal) cells was much weaker than that in the medial (ventral) cells. This tendency later became even clearer (stage 23, Figs. 2G and 2H). Chick Zic proteins were not detected in cells expressing Lim1/2 (Fig. 2J), a homeodomain protein expressed only in the neuronal subpopulation destined to become dorsal interneurons, nor in cells expressing βIII tubulin (data not shown), which is expressed in neuronal cells after their primary differentiation (Yaginuma *et al.,* 1990). The dorsal population of these cells coincided with Msx1/2-expressing cells (Fig. 2I). As a consequence, *Zic*-expressing dorsal neural cells may represent neural precursor cells before a certain stage of differentiation.

Dorsally Restricted Expression Is Regulated by Shh and BMPs

To understand how *CZic1* expression is limited to the dorsal region, we first examined the relation between notochord and *CZic1* expression. Notochord exerts ventralizing action on the spinal cord (Yamada *et al.,* 1991). When an additional notochord was transplanted to the site near the dorsal neural tube at stage 10 or 11, thinning of the neural wall was observed in proximity to the transplanted noto-
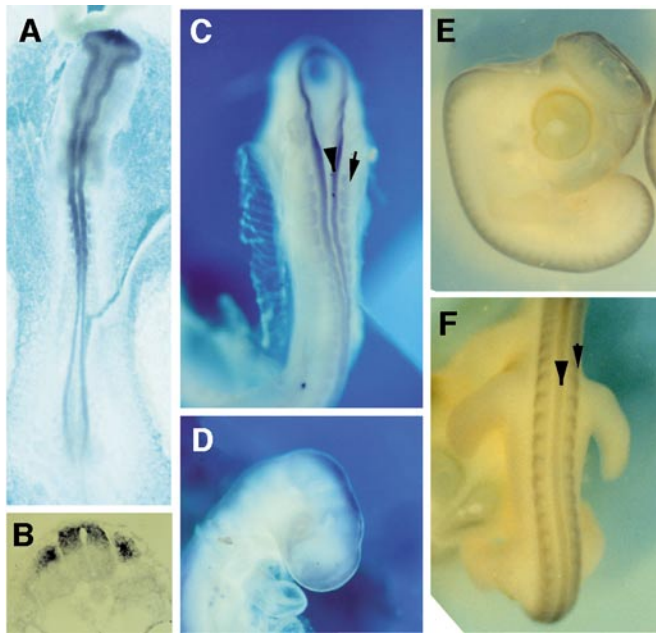
FIG. 1. Expression of *CZic1* as determined by *in situ* hybridization. Whole-mount preparation (A) and section (B) at the thoracic level of stage 10 embryos showing *CZic1* expression. This expression was recognized in the dorsal neural tube along almost the entire rostrocaudal extent and dorsomedial aspects of the somites. At stage 17, *CZic1* is strongly expressed in the dorsal hindbrain, spinal cord (C) midbrain and forebrain (D). Lateral (E) and dorsal (F) views of stage 23 embryos. Expression was restricted to the somites and the dorsal central nervous system. Arrowheads and arrows in (C) and (F) indicate staining of the dorsal neural tube and somites, respectively.

chord, which mimics a floor plate structure. With this change, the ventral border of the *Zic* expression are shifted dorsally on the transplanted side (Figs. 3A and 3B).

We then misexpressed *Shh* hemilaterally. To this end, the *Shh* expression plasmid vector was transfected by *in ovo* electroporation into the caudal end of the closing neural tube at stage 10. This condition allows us to misexpress *Shh* at various stages of spinal cord differentiation since the misexpression extends rostrocaudally where various stages of neural tube development have been observed. As expected, ectopic *Shh* expression caused a thinning of the neural tube in the caudal area (Figs. 3C and 3D), whereas misexpression in the rostral (more differentiated) region resulted in the generation of Islet1- and Islet2-positive motor neurons (data not shown). Chick Zic proteins were not detected in the vicinity of the *Shh*-expressing region (arrowhead in Fig. 3C). We therefore considered the inhibitory factor from the notochord to possibly be Shh itself.

We next examined the misexpression of secretory factors belonging to the TGFβ superfamily. Among these factors, we chose BMP4 and BMP7, since their effects on dorsal specification of the neural tube have been characterized.

Strong misexpression of both factors results in cell death and the subsequent disappearance of neural walls on the misexpressed side (data not shown) as described (Golden *et al.,* 1999). Near the missing neural wall sites, we observed
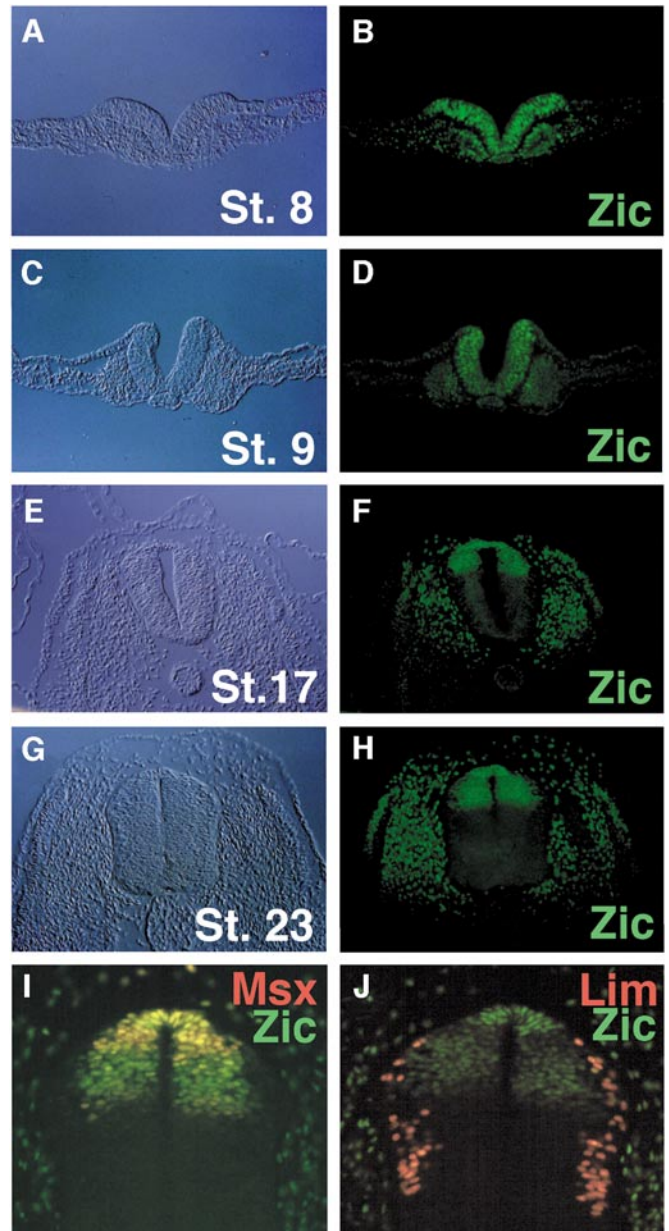

FIG. 2. Zic proteins are located in dorsal undifferentiated neural cells in the chick spinal cord. Immunohistochemical detection of Zic proteins (B, D, F, H, shown in green), and bright field views (A, C, E, G) in stage 8 (A, B), 9 (C, D), 17 (E, F), and 23 (G– J) embryos. (I, J) Double immunohistochemical staining showing the localization of Zic (green) and Msx1/2 proteins (red) (I) or Zic (green) and Lim1/2 proteins (red) (J). Msx1/2 proteins are detected in the same cells as Zic. The staining is therefore yellow.
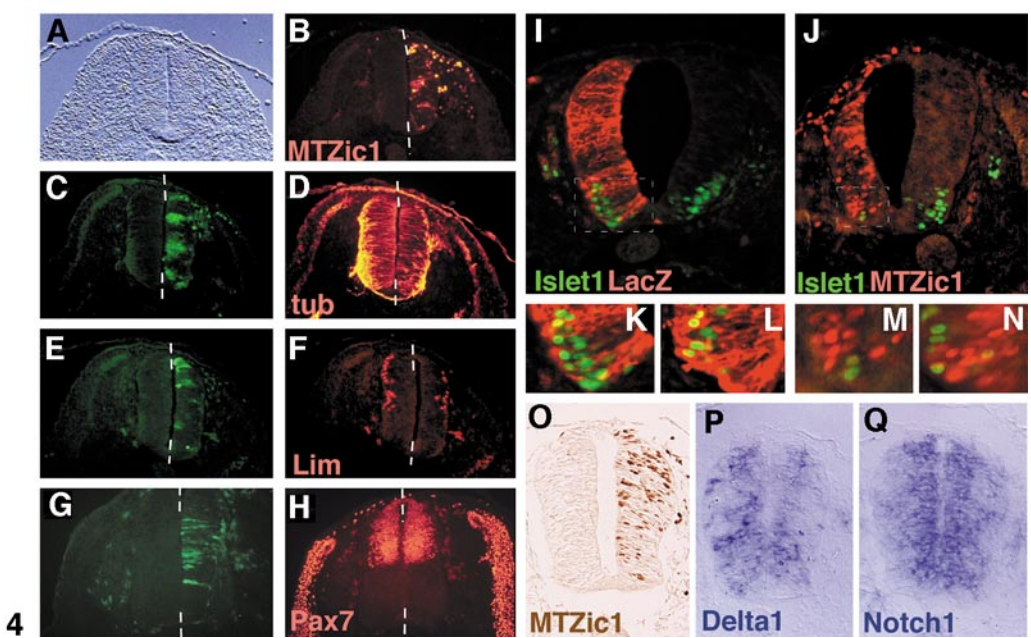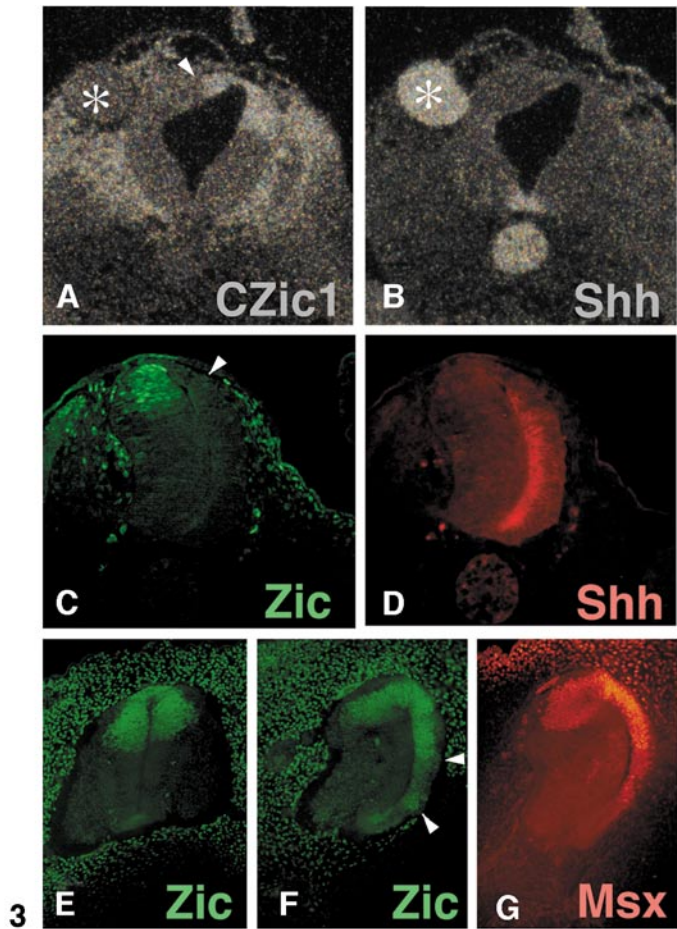
an ectopic localization of Zic proteins on the ventral side. The induction of Zic proteins occurred in a region of Msx1/2 induction (Figs. 3F and 3G). *Msx1/2* is normally expressed in roof plate cells, which also express *Zic* (Fig. 2I). Since Msx1/2 is induced by BMP signals (Vainio *et al.,* 1993; Suzuki *et al.,* 1997), our results indicated that Zic proteins are induced as a consequence of *BMP* misexpression.

Zic1 Misexpression Inhibits Neuronal Differentiation Irrespective of Its Location

Our next step was to clarify the role of Zic1 protein in the developing spinal cord. For this purpose, a Myc epitope-tagged CZic1 protein (MTZic1) expression vector was electroporated at stage 10 to misexpress *CZic1* on the ventral side. The spinal cord was examined 48 h later (stage 24). Transverse sections through the misexpressed site were stained with antibodies against molecular markers.

Cells expressing differentiated neural markers were found to be significantly affected by misexpression. Numbers of laterally located cells expressing *βIII tubulin*, which is expressed in these cells after primary neuronal differentiation, were significantly decreased on the misexpressed side (Figs. 4C and 4D). Consistent with this, the cells expressing *Lim1/2* (Figs. 4E and 4F) or *Islet1* (Figs. 4J, 4M and 4N) were decreased on the transfected side. Cells expressing these markers represent differentiated neuronal cells. *Lim1/2* was expressed in the dorsally located interneurons (Liem *et al.,* 1997). Islet1 is reportedly expressed in ventral motoneurons (Roelink *et al.,* 1995). These results led us to hypothesize that the misexpressed *CZic1* inhibited neuronal differentiation irrespective of its location along the dorsoventral axis. In contrast to the markers indicating progression of neuronal differentiation, the dorsoventral expressions of *Pax7* (Figs. 4G and 4H) and *Pax6* (data not shown) were not changed by MTZic1. This finding indicated the dorsoventral property, which is represented by Pax gene expressions not to be disturbed by Zic1.

To confirm neuronal differentiation inhibition by MTZic1, we next performed double labeling on the MTZic1 or LacZ expression vector-transfected embryos. The transfected spinal cords were immunohistochemically stained to detect either the MTZic1/Islet1 (Figs. 4I, 4K, and 4L) or the LacZ/Islet1 (Figs. 4J, 4M, and 4N). In the control *LacZ*-transfected embryos, the number of *Islet1*-expressing cells was 88.3% of that on the contralateral untransfected side (in 44 sections derived from 5 embryos). This slight reduction may reflect a toxic effect of electroporation-mediated plasmid transfection. In contrast, the Islet1-positive cells were reduced in the *MTZic1*-tranfected embryos (37.7% of the control side in 23 sections from 4 embryos). No *Zic1*-expressing cells expressed *Islet1*, among more than 1000 Zic1-positive cells located in the presumptive motor neuron-generating region, whereas LacZ/Islet1-positive cells were abundant in each section (Figs. 4K–4N). This result supports the idea that MTZic1 has the ability to inhibit neuronal differentiation.

We further examined the expression of *Notch1* and its ligand, *Delta1*, which constitute an established neuronal differentiation inhibitory system. As a result, *Notch1* expression was ectopically induced by the *MTZic1*-expressing side (Fig. 4Q), whereas *Delta1* expression was down-regulated in the *MTZic1*-expressing region (Fig. 4P). This result suggests that inhibition of neuronal differentiation by *MTZic1* is related to the Notch-Delta system.

Dorsal Neural Cells Were Increased in the Zic1-Overexpressing Transgenic Mouse

With misexpression, we occasionally observed a hyperplastic change in the *MTZic1* misexpressed site. However, the change was not consistent in an adequate number of embryos. We considered electroporation of the plasmids to not be suitable for the analysis of cell proliferation due to its transient expression profile and the presumptive cytotoxic effect. We therefore assessed the *Zic1* gene overdosage

FIG. 3. Zic gene expression regulation in the spinal cord. (A,B) The effects of notochord transplantation on the distributions of Zic1 (A) and Shh (B) transcripts. Transplanted notochord is indicated by an asterisk. The ventral border of the Zic1 expression area is shifted dorsally (arrowhead). (C, D) Effects of Shh misexpression on Zic proteins. Localization of Zic proteins (green in C) and Shh protein (red in D) is shown in a section through the lumbar spinal cord, where the Shh expression vector was introduced into the right side of the spinal cord. Zic proteins disappeared on the Shh-misexpressing side (arrowhead). (E–G) BMP4 and BMP7 are misexpressed (F, G) or not (E) on the right side of the spinal cord. Sections through the thoracic spinal cord showing the localization of Zic proteins (green in E, F) and Msx proteins (red in G). Note that Zic and Msx1/2 proteins were induced on the ventral side by the misexpression (arrowheads).

FIG. 4. Misexpression of *MTZic1* in the developing chick spinal cord. The pictures show transverse sections from *EF-MTZic1* (A–H, J, M–Q) or *EF-LacZ* (I, K, L)-electroporated spinal cords. Misexpression is present on the right side of the spinal cord. Vertical broken lines indicate the right to left border of the area of misexpression. (A) Bright field differential views. (C, E, G) Localization of GFPs, which are coexpressed with MTZic1, is indicated in green. (B), (D), (F), and (H) are taken from the same sections as (A), (C), (E), and (G), respectively. Red staining shows the immunohistochemical localization of MTZic1 (B), βIII tubulin (D), Lim1/2 (F), and Pax7 (H). (I–N) Double labeling with LacZ (red) and Islet1 (green) (I, K, L), or MTZic1 (red) and Islet1 (green) (J, M, N). (K) and (M) are higher magnification views of (I) and (J), respectively. (L) and (N) are other examples of double labeling (higher magnification view). In (K–N), yellow color indicates doubly labeled cells which were found with the *LacZ* misexpression (K, L), but not in the *MTZic1* misexpression (M, N). (O–Q) Serial adjacent sections showing the distribution of MTZic1 protein (O), Delta1 (P) mRNA, and Notch1 (Q) mRNA. *Delta1* expression is reduced, whereas the *Notch1* expression is ectopically induced in the misexpressed side.

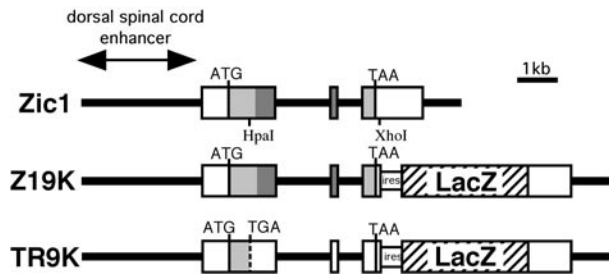**FIG. 5.** Zic1-overexpressing transgenic constructs. The wild-type *Zic1* gene consists of three exons. The proximal 2.9-kb promoter is sufficient for dorsal spinal cord expression. The light gray box indicates the protein-coding region. The dark gray box indicates the zinc finger domain. The *Z19K* construct contains intact ORF. The *TR9K* construct contains a termination codon in the amino-terminal region of the ORF and does not produce intact protein. Both constructs carry an ires-LacZ cassette to monitor transgene expression.

effect on spinal cord development by generating transgenic mice carrying additional *Zic1* genes. For this purpose, we used a 9-kb region containing the entire protein-coding region of mouse *Zic1* and its dorsal spinal cord enhancer, which lies in the proximal 2.9 kb of the *Zic1* 5′ flanking region (Aruga *et al.,* 2000). Two kinds of transgenes were prepared to evaluate the role of Zic1 protein (Fig. 5). One contained the intact protein coding region (*Z19K*) and the other contained a stop codon (*TR9K*) in an amino-terminal region of the Zic1 protein. Both constructs contained an ires-LacZ cassette in the 3′ noncoding region to show the transgene expression.

Two *Z19K* and one *TR9K* transgenic mouse lines were established. We examined the thoracic spinal cord phenotype at E11, E14, and E15. No clear difference was observed at E11 (data not shown). However, at E15, *Z19K* mice showed significant hypercellularity in the dorsal region (Fig. 6D). The cellular mass of the dorsal horn was extruded laterally and the dorsoventral extent of the posterior funiculus was generally reduced. *TR9K* mice were indistinguishable from wild-type spinal cord at the same stage (data not shown). To illustrate the difference more clearly, the transgene-expressing cells were detected by anti-LacZ staining. The stained cells were more densely packed in the dorsal spinal cord of the two *Z19K* murine lines than in the

TR9k line (Figs. 6B, 6C, 6E, and 6F). This observation result indicates that overexpressed *Zic1* enhanced the generation of neural precursors in the dorsal spinal cord.

A marker study of the E14 spinal cord revealed the preceding molecular events in the *Z19K* spinal cord. *Notch1* was enhanced and extended expression laterally in the dorsal ventricular zone where the transgene was over-expressed (Figs. 6H, 6J, and 6K). The *Notch1*-enhanced region also showed increased expression of *Hes1*, which encodes a transcription factor downstream of Notch-mediated signaling (Figs. 6I and 6L). Therefore, *Zic1* was considered to activate the Notch signaling cascade, which corresponded to the results of the misexpression experiment using chick spinal cord.

### Cell Number Was Decreased in Dorsal Spinal Cord of the Zic1-Deficient Mouse

To further confirm the above hypothesis, we examined the spinal cord phenotype of the *Zic1* mutant mouse (Aruga *et al.,* 1998). In mice homozygous for the *Zic1* null type mutation ($Zic1^{-/-}$), the most obvious abnormalities were in the cerebellum, which is derived from the dorsal hindbrain. The abnormality is characterized by hypoplasia and abnormal foliation patterns (Aruga *et al.,* 1998). Other neural abnormalities have not yet been described.

Since the spinal cord of $Zic1^{-/-}$ appeared normal at birth on histological examination, a morphometric analysis was done on the thoracic spinal cords of the E15 embryos. As we expected, a spinal cord comparison revealed a difference between ($Zic1^{+/+}$, $Zic1^{+/-}$) and $Zic1^{-/-}$. In $Zic1^{-/-}$, the dorsal horn mass was decreased (Figs. 7A and 7B). To compare the areas of the dorsal region, we measured these areas by employing digitized images. The dorsal cell mass reduction was shown to be significant (see figure legend to Fig. 7).

We questioned whether these changes might involve disturbances in differentiation, and examined differentiation markers in the mutant spinal cord at E11.5. Neuronal differentiation markers, βIII tubulin, and dorsal and ventral spinal cord markers (Math1, Pax6, Pax7, Lim1/2, Islet1, Msx1/2) were examined in the $Zic1^{-/-}$ spinal cord. Essentially, all of the marker-expressing cells were detected at essentially the same levels as in wild-type littermates, except that the number of the most dorsal neuronal progenitors expressing *Math1* was decreased (Msx2, Figs. 7E and 7F; Math1, Figs. 7G and 7H; others, data not shown).

FIG. 6. Spinal cord phenotype of the *Zic1*-overexpressing transgenic mouse. Transverse sections of the thoracic spinal cord of E15 (A–F) and E14 (G–L) wild-type (A), *Z19K* (D–F, K, L), and *TR9K* (B, C, G–J) mice. (A, D) Hematoxylin-eosin stain. Arrows in D indicate characteristic lateral extrusion of cellular mass of the dorsal horn. This picture is from the a *Z19K* line specimen, the other lines showed similar changes (data not shown). The asterisk indicates the prospective dorsal funiculus, which is thin in the *Z19K* transgenic mouse. (B, C, E, F, J) Immunohistochemical staining with anti-LacZ antibody. (C) and (F) are higher magnifications of (B) and (E), respectively. The *Z19K* spinal cord shows hypercellularity in the dorsal horn. (H, I, K, L) *In situ* hybridization showing the distribution of Notch1 mRNA (H, K) and Hes1 mRNA (I, L). *Notch1* and *Hes1* expressions are both enhanced in the *Z19K* dorsal ventricular zone (arrowheads).
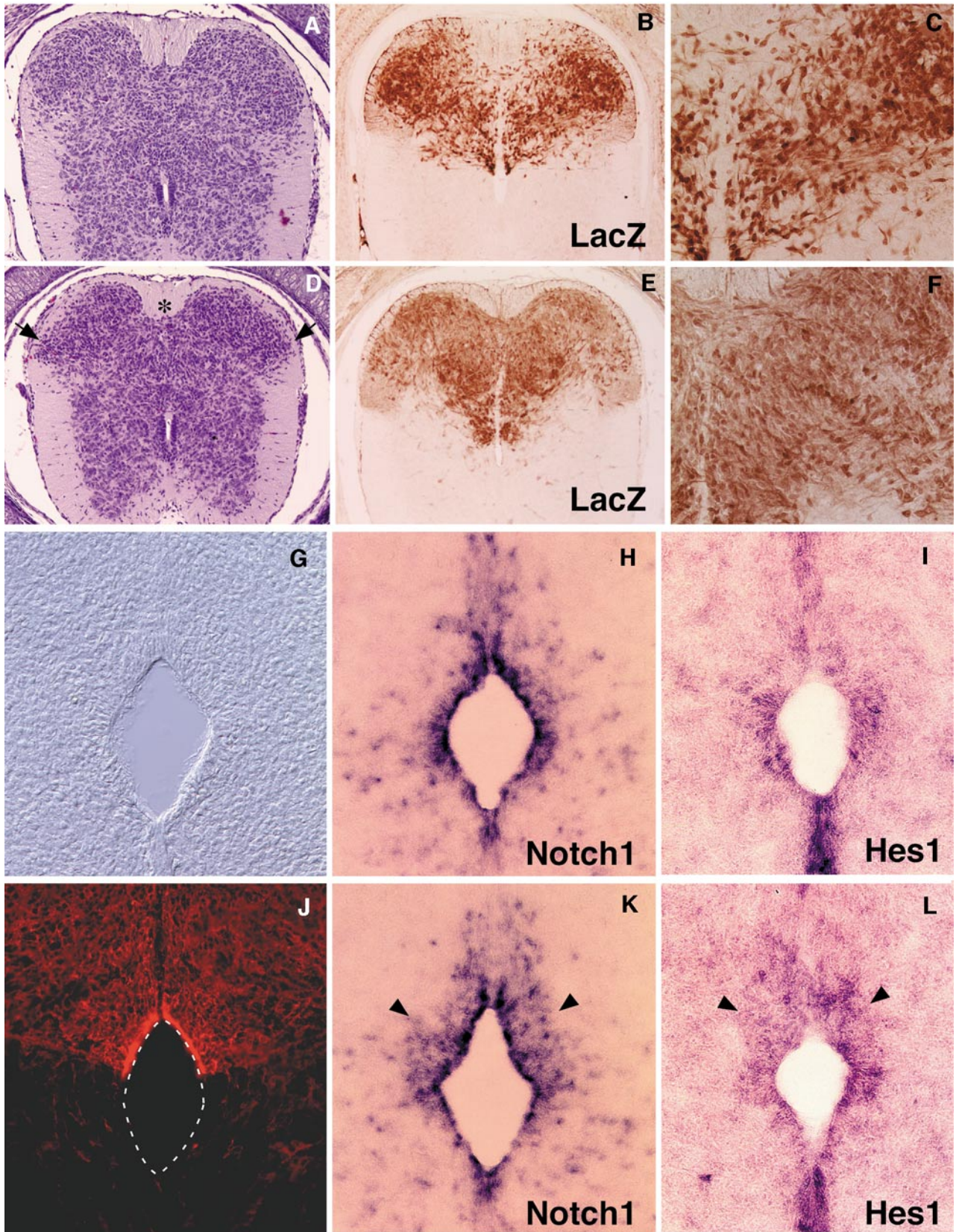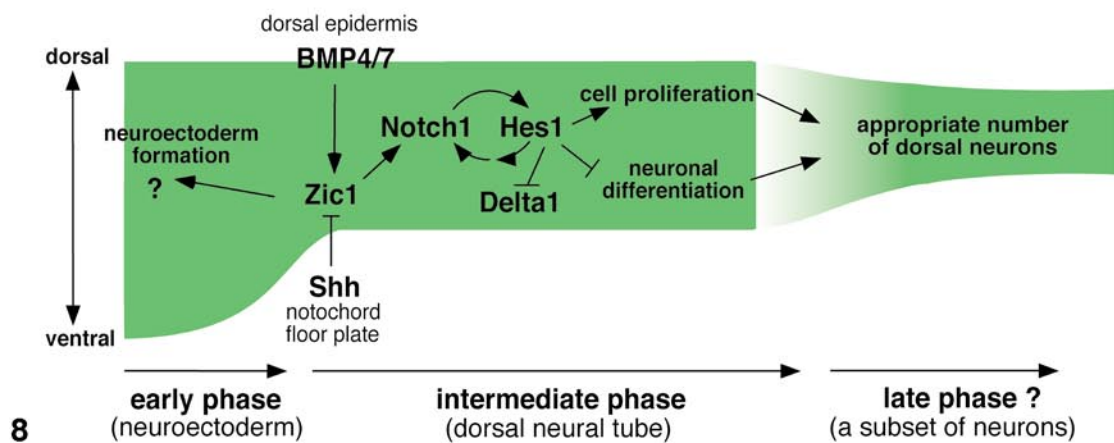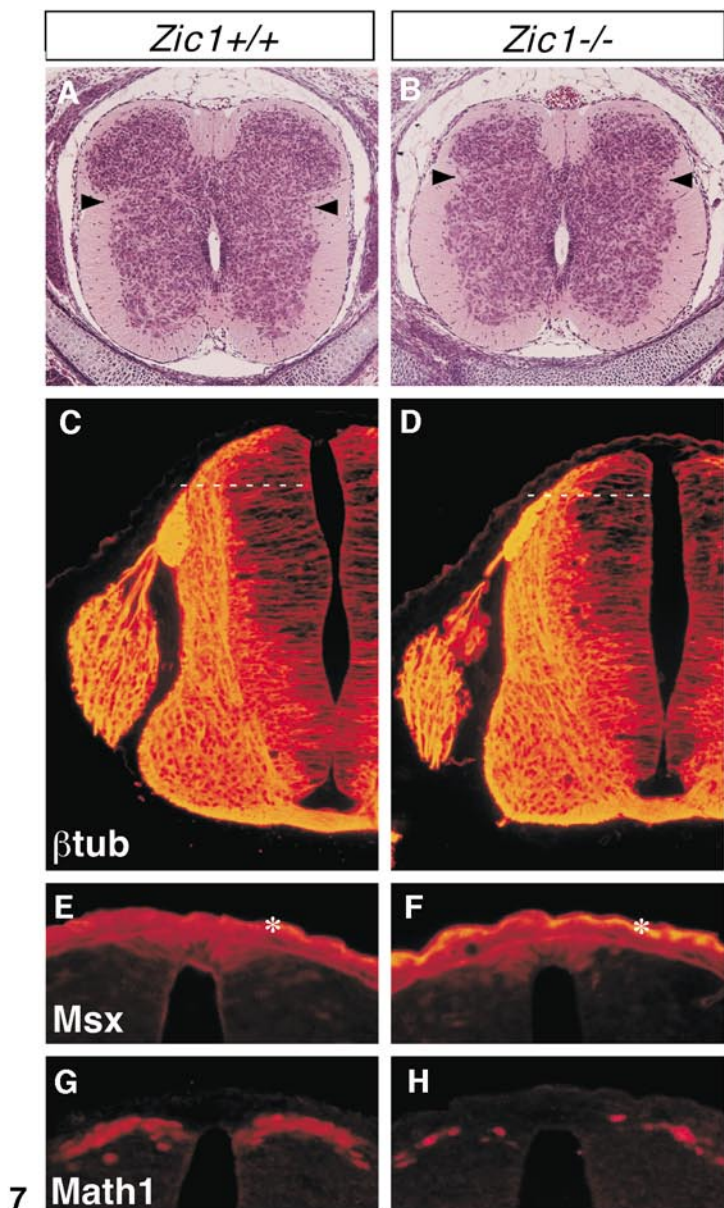
Correspondingly, the dorsal ventricular cell mass was smaller in $Zic1^{-/-}$ (data not shown). The thickness of the βIII tubulin-stained cell layer in the dorsal region was generally increased, suggesting premature neuronal differentiation (Figs. 7C and 7D). These are the earliest abnormalities found in $Zic1^{-/-}$, to date. The cell death frequency was not changed in either $Zic1$-deficient mice or $Zic1$-overexpressing mice (data not shown). As a consequence, the loss-of-function phenotype as well as the gain-of-function phenotype also supported the idea that $Zic1$ promotes the expansion of dorsal neural progenitors without qualitatively changing dorsoventral neural property.

DISCUSSION

Regulation of Zic Gene Expression in the Dorsal Spinal Cord

$CZic1$ and almost all other Zic genes are expressed, to some extent, in the dorsally restricted region of the spinal cord in chick, mouse, frog, and fish embryos (Nagai *et al.*, 1997; Nakata *et al.*, 1997, 1998; Mizuseki *et al.*, 1998; Kuo *et al.*, 1998; Brewster *et al.*, 1998; Grinblat *et al.*, 1998), suggesting that gene expression regulation is conserved among Zic family members. This study revealed a regulatory mechanism involved in $CZic1$ expression.

First, we showed that Shh has an inhibitory effect on $Zic1$ expression *in vivo*. The results of a notochord transplantation experiment were consistent with those of $Zic1$ and $Zic2$ expressions in $Wnt3a$ mutant mice (Nagai *et al.*, 1997; Takada *et al.*, 1994). In the mutant mice, the ventral border of the $Zic1$ and $Zic2$ expression area in the spinal cord shifted ventrally when the notochord degenerated and disappeared. Thus, the presence of notochord is involved in the dorsally restricted expression of Zic genes.

Shh protein is detectable in the chick spinal cord slightly earlier than at the eight-somite stage (ca. stage 9), initially in the midbrain. Expression extends rostrally and caudally and reaches the fifth somite level by stage 10 (Marti *et al.*, 1995). Zic proteins become dorsally restricted, which coincides with Shh expression. These results, taken together with those of the Shh-misexpression experiment, suggest that Shh proteins suppress Zic expression in the ventral spinal cord during the normal course of the development.

A second finding concerning regulation is that misexpressions of BMP4 and BMP7 induced expression of the Zic genes. BMPs are known to be involved in the induction of neural crest and roof plate differentiation by epidermal ectoderm (Dickinson *et al.*, 1995; Liem *et al.*, 1995, 1997; Lee *et al.*, 1998). A recent study showed $Zic1$ to be induced in mesencephalon/metencephalon explants, by both BMP7 and GDF7, which are expressed in this region (Adler *et al.*, 1999). This finding is consistent with ours and suggests that a similar regulatory mechanism exists in the neural tube all along the rostrocaudal axis.

However, a temporal change in the regulation of Zic genes by BMPs should be noted. This is because, in the ectoderm, $Xenopus$ $Zic3$ is induced by blockade of the BMP signal at the initial phase of neural plate formation (Nakata *et al.*, 1997, 1998). Although the regulation of $CZic1$ by BMPs at the corresponding stage is not fully understood, a similar regulatory mechanism may underlie $CZic1$ expression. Since CZic1 is detectable just after the neuroectoderm formation (unpublished observation) and is evenly expressed along the dorsoventral axis (Fig. 3), the induction of CZic1 by misexpressed BMPs may reflect the role for BMPs in a later phase of development. BMPs may be principally involved in the maintenance of dorsal Zic expression in the neural tube.

The Role of Zic1 in Spinal Cord Development

Gain-of-function analysis. We previously overexpressed $Xenopus$ Zic genes in the $Xenopus$ embryo (Nakata *et al.*, 1997, 1998). In these experiments, the neural plate was enlarged on the overexpressed side, while further neuronal differentiation, as determined by N-tubulin expression, varied considerably and was often inhibited (K. Nakata, J.A., K.M., unpublished observation). This variation may reflect a difference in the temporal profile of

---

FIG. 7. Spinal cord phenotype of $Zic1$-deficient mice. (A, B) Hematoxylin-eosin-stained transverse sections of thoracic spinal cord from $Zic1^{+/+}$ (A) and $Zic1^{-/-}$ (B). Arrowheads indicate the arbitrary ventral borders of the dorsal horn used to measure the area of the dorsal horn. The areas were 75 ± 5 ($Zic1^{+/+}$), 75 ± 8 ($Zic1^{+/-}$), and 55 ± 11 ($Zic1^{-/-}$) arbitrary units based on measurements on four sets of the three genotypes derived from four independent litters. (C–H) Immunohistochemical staining of the spinal cord from $Zic1^{+/+}$ (C, E, G) and $Zic1^{-/-}$ (D, F, H) at E11.5. Antibodies against βIII tubulin (C, D), Msx1/2 (E, F), and Math1 (G, H) were used for this study. The area containing the undifferentiated neural cells in the most dorsal region (the dark region above the broken line in C and D) is decreased in $Zic1^{-/-}$. Msx-expressing roof plate cells exist in both $Zic1^{+/+}$ and $Zic1^{-/-}$ (E, F). $Math1$-expressing dorsal neuronal progenitors were detected in both genotypes, but the number was decreased in $Zic1^{-/-}$ (G, H). The epidermal staining indicated by asterisks in (E) and (F) is nonspecific, and is observed even in the absence of the primary antibody.

FIG. 8. A model illustrating the involvement of Zic1 in the spinal cord development. The ordinate indicates the dorsoventral axis in neural tissue. The abscissa indicates the developmental stages. The green area indicates the $Zic1$-expressing region.

misexpression. mRNA injection into young *Xenopus* embryos does not have a long-lasting effect on expression in many cases. It is not clear whether the overexpressed proteins are substantially maintained until the neuronal differentiation stage. In the chick electroporation system, however, expression of the introduced gene can be detected as early as 2 h after *in ovo* electroporation, and the strongly expressed state continues for 24–48 h (Funahashi *et al.,* 1999). Therefore, we could misexpress *Zic1* during neural tube formation, much later than in the *Xenopus* system. As a consequence, misexpression in chick spinal cord revealed the function of Zic1 protein in neuronal differentiation, but not in neuroectoderm differentiation (neural plate formation).

Zic1 overexpression using transgenic mice also allows evaluation of the role of *Zic1* in the corresponding stage because transgene expression is detectable after E8.5 (Aruga *et al.,* 2000; data not shown) when neuroectoderm differentiation has already been completed. Since we established transgenic lines, it is possible that embryos with a more severe phenotype, which may result in embryonic death, were lost in this study. In addition, the apparent absence of major behavioral abnormalities in several adult *Z19K* transgene founder mice suggests that the gene-overdosage effect is not detrimental to either postnatal development or mature functioning of the spinal cord.

Loss-of-function analysis. In the spinal cords of *Zic1*-deficient mice, we observed a significant decrease in dorsal horn mass at E15. This result can be considered in relation to the cerebellar abnormality seen in these mice. In the developing *Zic1*-deficient cerebellum, cell proliferation is decreased in external germinal layer (EGL) cells, where *Zic1* is expressed (Aruga *et al.,* 1994, 1998) during embryonic development. It is intriguing that EGL cells are derived from the upper (rostral) rhombic lip, originally located in the dorsal most part of the hindbrain. In *Zic1*$^{-/-}$, we also recognized decreases in cell numbers of the pontine and inferior olivary nuclei (data not shown), which are known to migrate from the lower (caudal) rhombic lip (Altman and Bayer, 1997). Therefore, the neural abnormality in the *Zic1*-deficient mice can be characterized as a general reduction of cell numbers in dorsal neural tube derivatives in the hindbrain and spinal cord.

How about other *Zic* mutants? *Zic2* knockdown mutants are characterized by impaired dorsal forebrain development and insufficient closure of the posterior neuropore (Nagai *et al.,* 2000). *Zic3*-deficient embryos frequently show exencephaly in the hindbrain (Klootwijk *et al.,* 2000; Carrel *et al.,* 2000). Recently, we found a cerebellar abnormality, very similar to that in *Zic1*$^{-/-}$, in *Zic1/Zic2* trans-heterozygotes (*Zic1*$^{+/-}$, *Zic2*$^{+/-}$) (Aruga *et al.,* 2002). This observation indicates that the functions of Zic1 and Zic2 are similar in the developing cerebellum. Therefore, it is possible that the neural tube abnormalities in Zic2 and Zic3 are attributable to reduced cell numbers in dorsal neural tissues, especially in light of the functional similarities among Zic1, Zic2, and Zic3 as transcription factors (Mizugishi *et al.,* 2001; Koyabu *et al.,* 2001).

Zic1 Inhibits Neuronal Differentiation by Activating Notch Signaling

All three types of *Zic1*-manipulating experiments indicated that Zic1 inhibits neuronal differentiation. As a mechanism of neuronal differentiation inhibition, current results suggest the involvement of Notch signaling. Notch signaling is an evolutionarily conserved mechanism that controls differentiation and proliferation of many tissues (reviewed by Weinmaster, 1997; Artavanis-Tsakonas *et al.,* 1999). Cell–cell interactions between Notch ligand Delta-expressing and Notch-expressing cells lead to activation of Notch signaling in receiving cells. Ligand activation of Notch is transduced to activate transcription of Hes1 and other transcription factor genes that downregulate the expression of *Delta* and upregulate expression of the *Notch*. Thus, Notch signaling is considered to act as a positive feedback system regulating its own expression. Since Zic1 enhanced *Notch1* and *Hes1* expression and suppressed *Delta1* expression, Zic1 may strengthen this positive feedback loop. Considering its transcriptional activator function, it is likely that Zic1 positively regulates the expression of *Notch1* or *Hes1*, or both.

A recent study showed that activated Notch2 signaling inhibits differentiation of cerebellar granule cell precursors in the EGL (Solecki *et al.,* 2001). On the other hand, we recently found that premature differentiation occurs in *Zic1*-deficient and *Zic1/Zic2* compound mutant cerebella (Aruga *et al.,* 2002). These two lines of evidence raise the possibility that Zic1 also controls the Notch signaling in the cerebellum. Accordingly, Notch regulates a cell cycle controlling gene, *cyclin D1*, which is downregulated in both of the *Zic* mutant cerebella (Ronchini and Capobianco, 2001; Aruga *et al.,* 2002).

Although the role of Notch signaling has not been demonstrated in developing chick and mouse spinal cords, it has been shown that overexpressed extracellular deletion of the *Xenopus* Notch homologue inhibits primary neuronal differentiation, which occurs in the spinal cord forming region of the frog embryo (Coffman *et al.,* 1993). It is probable that the Zic1-mediated neuronal differentiation in the spinal cord is due to Notch signaling activation. However, additional problems remain to be resolved before a comprehensive understanding of the link between Zic and Notch signaling can be achieved. First, recent studies raised the possibility that Notch signaling acts instructively to promote gliogenesis (reviewed by Wang and Barres, 2000). The gliogenesis in *Zic1*-manipulated neural tissue warrants examination. Second, the involvement of other Zic family genes in the control of Notch signaling must be clarified. Third, it would be interesting to examine whether the Zic-Notch link can act in situations other than spinal cord development.

CONCLUSION

In conclusion, the involvement of *Zic1* in spinal cord development may be summarized as follows (Fig. 8). First, *Zic1* is expressed in the neural plate inherent to undifferentiated neural tissue. Then, Shh represses *Zic1* expression in the ventral part of the neural tube, and BMP4 and BMP7 maintain the dorsal *Zic1* expressions. Exclusion of the Zic1 protein may allow for earlier neuronal differentiation of ventral cells. In the dorsal spinal cord, Zic1 promotes the expansions of neural cells by activating Notch signaling. As a consequence, Zic1 controls the number of dorsal neural progenitors at an appropriate level.

This summary requires us to assume that Zic1 has an unidentified function in the mature brain. We detected Zic proteins in cells located in the dorsal horn at adult stage (data not shown), despite expression having been diminished in the early phase of neuronal differentiation. This temporal expression profile is essentially conserved in the cerebellum. Mouse Zic1 is persistently expressed in cerebellar granule cell precursors at the embryonic stage, and this expression is reduced before differentiation prior to leaving the proliferative cell cycle, followed by reactivated expression in mature granule neurons (Aruga *et al.,* 1994, 2002; unpublished observation; Dahmane and Ruiz-i-Altaba, 1999). The role of Zic1 in adult neural tissue can be evaluated employing stage-specific genetic manipulation of experimental animals.

REFERENCES

Adler, J., Lee, K. J., Jessell, T. M., and Hatten, M. E. (1999). Generation of cerebellar granule neurons in vivo by transplantation of BMP-treated neural progenitor cells. *Nat. Neurosci.* **7,** 535–540.

Altman, J. A., and Bayer, S. A. (1997). Development of the precerebellar system. In "Development of the Cerebellar System," pp. 266–321. CRC Press, New York.

Artavanis-Tsakonas, S., Rand, M. D., and Lake, R. J. (1999). Notch signaling: Cell fate control and signal integration in development. *Science* **284,** 770–776.

Aruga, J., Yokota, N., Hashimoto, M., Furuichi, T., Fukuda, M., and Mikoshiba, K. (1994). A novel zinc finger protein, Zic, is involved in neurogenesis, especially in the cell lineage of cerebellar granule cells. *J. Neurochem.* **63,** 1880–1890.

Aruga, J., Nagai, T., Tokuyama, T., Hayashizaki, Y., Okazaki, Y., Chapman, V. M., and Mikoshiba, K. (1996). The mouse Zic gene family: Homologues of Drosophila pair-rule gene odd-paired. *J. Biol. Chem.* **271,** 1043–1047.

Aruga, J., Minowa, O., Yaginuma, H., Kuno, J., Nagai, T., Noda, T., and Mikoshiba, K. (1998). Mouse Zic1 is involved in cerebellar development. *J. Neurosci.* **18,** 284–293.

Aruga, J., Shimoda, K., and Mikoshiba, K. (2000). A 5′ segment of the mouse Zic1 gene contains a region specific enhancer for dorsal hindbrain and spinal cord. *Mol. Brain Res.* **78,** 15–25.

Aruga, J., Inoue, T., Hoshino, J., and Mikoshiba, K. (2002). Zic2 controls the cerebellar development in cooperation with Zic1. *J. Neurosci.* **22,** 218–225.

Benedyk, M. J., Mullen, J. R., and DiNardo, S. (1994). odd-paired: A zinc finger pair-rule protein required for the timely activation of engrailed and wingless in Drosophila embryos. *Genes Dev.* **8,** 105–117.

Brewster, R., Lee, J., and Ruiz-i-Altaba, A. (1998). Gli/Zic factors pattern the domain of neural plate by defining domains of cell differentiation. *Nature* **393,** 579–583.

Carrel, T., Purandare, S. M., Harrison, W., Elder, F., Fox, T., Casey, B., and Herman, G. E. (2000). The X-linked mouse mutation Bent tail is associated with a deletion of the Zic3 locus. *Hum. Mol. Genet.* **9,** 1937–1942.

Coffman, C. R., Skoglund, P., Harris, W. A., and Kintner, C. R. (1993). Expression of an extracellular deletion of Xotch diverts cell fate in Xenopus embryos. *Cell* **73,** 659–671.

Dahmane, N., and Ruiz-i-Altaba, A. (1999). Sonic hedgehog regulates the growth and patterning of the cerebellum. *Development* **126,** 3089–3100.

Dickinson, M. E., Selleck, M. A. J., McMahon, A. P., and Bronner-Fraser, M. (1995). Dorsalization of the neural tube by the non-neuronal ectoderm. *Development* **121,** 2099–2106.

Dubreuil, V., Hirsch, M., Pattyn, A., Brunet, J., and Goridis, C. (2000). The Phox2b transcription factor coordinately regulates neuronal cell cycle exit and identity. *Development* **127,** 5191–5201.

Echelard, Y. Epstein, D. J., St-Jacques, B., Shen, L., Mohler, J., McMahon, J. A., and McMahon, A. P. (1993). Sonic hedgehog, a member of a family of putative signaling molecules, is implicated in the regulation of CNS polarity. *Cell* **75,** 1417–1430.

Funahashi, J.-i., Okafuji, T., Ohuchi, H., Noji, S., Tanaka, H., and Nakamura, H. (1999). Role of Pax-5 in the regulation of a midhindbrain organizer's activity. *Dev. Growth. Differ.* **41,** 59–72.

Golden, J. A., Bracivolovic, A., Mcfadden, K. A., Beesley, J. S., Rubenstein, J. L. R., and Grinspan, J. B. (1999). Ectopic bone morphogenetic proteins 5 and 4 in the chicken forebrain lead to cyclopia and holoprosencephaly. *Proc. Natl. Acad. Sci. USA* **96,** 2439–2444.

Grinblat, Y., Gamse, J., Patel, M., and Sive, H. (1998). Determination of the zebrafish forebrain: Induction and patterning. *Development* **125,** 4403–4416.

Helms, A. W., and Johnson, J. E. (1998). Progenitors of dorsal commissural interneurons are defined by MATH1 expression. *Development* **125,** 919–928.

Hamburger, V., and Hamilton, H. L. (1951). A series of normal stages in the development of chick embryo. *J. Morphol.* **88,** 49–92.

Hui, C. -c., Slusarski, D., Platt, K. A., Holmgren, R., and Joyner, A. L. (1995). Expression of three mouse homologs of the Drosophila segment polarity gene cubitus interruptus, Gli, Gli-2, and Gli-3, in ectoderm and mesoderm-derived tissues suggests multiple roles during postimplantation development. *Dev. Biol.* **162,** 402–413.

Jang, S. K., Davies, M. V., Kaufman, R. J., and Wimmer, E. (1989). Initiation of protein synthesis by internal entry of ribosomes into the 5′ nontranslated region of encephalomyocarditis virus RNA in vivo. *J. Virol.* **63,** 1651–1660.

Klootwijk, R., Franke, B., van der Zee, C. E. E. M., de Boer, R. T., Wilms, W., Hol, F. A., and Mariman, E. C. M. (2000). A deletion encompassing *Zic3* in Bent tail, a mouse model for X-linked neural tube defects. *Hum. Mol. Genet.* **9,** 1615–1622.

Koyabu, Y., Nakata, K., Mizugishi, K., Aruga, J., and Mikoshiba, K. (2001). Physical and functional interaction between Zic and Gli proteins. *J. Biol. Chem.* **276,** 6889–6892.

Kuo, J. S., Patel, M., Gamse, J., Merzdorf, C., Liu, X., Apekin, V., and Sive, H. (1998). Opl: A zinc finger protein that regulates neural determination and patterning in Xenopus. *Development* **125,** 2867–2882.

Lee, K. J., Mendelsohn, M., and Jessell, T. M. (1998). Neuronal patterning by BMPs: A requirement for GDF7 in the generation of a discrete class of commissural interneurons in the mouse spinal cord. *Genes Dev.* **12,** 3394–3407.

Liem, K. F., Jr., Tremmi, G., Roelink, H., and Jessel, T. M. (1995). Dorsal differentiation of neural plate cells induced by BMP-mediated signals from epidermal ectoderm. *Cell* **82,** 969–979.

Liem, K. F., Jr., Tremml, G., and Jessell, T. M. (1997). A role for the roof plate and its resident TGFbeta-related proteins in neuronal patterning in the dorsal spinal cord. *Cell* **91,** 127–138.

Marti, E., Takada, R., Bumcrot, D. A., Sasaki, H., and McMahon, A. P. (1995). Distribution of Sonic hedgehog peptides in the developing chick and mouse embryo. *Development* **121,** 2537–2547.

Mizugishi, K., Aruga, J., Nakata, K., and Mikoshiba, K. (2001). Molecular properties of Zic proteins as transcriptional regulators and their relationship to GLI proteins. *J. Biol. Chem.* **276,** 2180–2188.

Mizuseki, K., Kishi, M., Matsui, M., Nakanishi, S., and Sasai, Y. (1998). Xenopus Zic-related-1 and Sox-2, two factors induced by chordin, have distinct activities in the initiation of neural induction. *Development* **125,** 579–587.

Mizushima, S., and Nagata, S. (1990). pEF-BOS, a powerful mammalian expression vector. *Nucleic Acids Res.* **18,** 5322.

Monaghan, A. P., Davidson, D. R., Sime, C., Graham, E., Baldock, R., Bhattacharya, S. S., and Hill, R. E. (1991). The Msh-like homeobox genes define domains in the developing vertebrate eye. *Development* **112,** 1053–1061.

Nagai, T., Aruga, J., Takada, S., Gunther, T., Sporle, R., Schughart, K., and Mikoshiba, K. (1997). The expression of the mouse Zic1, Zic2 and Zic3 gene suggests an essential role for Zic gene in body pattern formation. *Dev. Biol.* **182,** 299–313.

Nagai, T., Aruga, J., Minowa, O., Sugimoto, T., Ohno, Y., Noda, T., and Mikoshiba, K. (2000). Zic2 regulates the kinetics of neurulation. *Proc. Natl. Acad. Sci. USA* **97,** 1618–1623.

Nakata, K., Nagai, T., Aruga, J., and Mikoshiba, K. (1997). Xenopus Zic3, a primary regulator both in neural and neural crest. *Proc. Natl. Acad. Sci. USA* **94,** 11980–11985.

Nakata, K., Nagai, T., Aruga, J., and Mikoshiba, K. (1998). Xenopus Zic family and its role in neural and neural crest development. *Mech. Dev.* **75,** 43–51.

Roelink, H., Porter, J., Chiang, C., Tanabe, Y., Chang, D. T., Beachy, P. A., and Jessel, T. M. (1995). Floor plate and motor neuron induction by different concentrations of amino-terminal cleavage product of Sonic hedgehog autoproteolysis. *Cell* **81,** 445–455.

Ronchini, C., and Capobianco, A. J. (2001). Induction of cyclin D1 transcription and CDK2 activity by Notch(ic): Implication for cell ceble disruption in transformation by Notch(ic). *Mol. Cell. Biol.* **21,** 5925–5934.

Ruppert, J. M., Kinzler, K. W., Wong, A. J., Bigner, S. H., Kao, F.-T., Law, M. L., Seuanez, H. N., O'Brien, S. J., and Vogelstein, B. (1988). The GLI-Kruppel family of human genes. *Mol. Cell. Biol.* **8,** 3104–3313.

Sakamoto, K., Nakamura, H., Takagi, M., Takeda, S., and Katsube, K. (1998). Ectopic expression of lunatic Fringe leads to downregulation of Serrate-1 in the developing chick neural tube: Analysis using in ovo electroporation transfection technique. *FEBS Lett.* **426,** 337–341.

Sánchez-Garcia, I., and Rabbitts, T. H. (1994). The LIM domain: A new structural motif found in zinc-finger-like proteins. *Trends Genet.* **10,** 315–320.

Solecki, D. J., Liu, X. L., Tomoda, T., Fang, Y., and Hatten, M. E. (2001). Activated Notch2 signaling inhibits differentiation of cerebellar granule neuron precursors by maintaining proliferation. *Neuron* **31,** 557–568.

Suzuki, A., Ueno, N., and Hemmati-Brivanlou, A. (1997). Xenopus msx1 mediates epidermal induction and neural inhibition by BMP4. *Development* **124,** 3037–3044.

Stuart, E. T., Kioussim, C., and Gruss, P. (1994). Mammalian Pax genes. *Annu. Rev. Genet.* **28,** 219–236.

Takada, S., Stark, K. L., Shea, M. J., Vassileva, G., McMahon, J. A., and McMahon, A. P. (1994). Wnt-3a regulates somite and tailbud formation in the mouse embryo. *Genes Dev.* **8,** 174–189.

Turner, D. L., and Weintraub, H. (1994). Expression of acaete-scute homolog 3 in Xenopus embryos converts ectodermal cells to a neural fate. *Genes Dev.* **8,** 1434–1447.

Vainio, S., Karabanova, I., Jowett, A., and Thesleff, I. (1993). Identification of BMP-4 as a signal mediating secondary induction between epithelial and mesenchymal tissues during early tooth development. *Cell* **75,** 45–58.

Wang, S., and Barres, B. A. (2000). Up a Notch. Instructing gliogenesis. *Neuron* **27,** 197–200.

Weinmaster, G. (1997). The ins and outs of Notch signaling. *Mol. Cell. Neurosci.* **9,** 91–102.

Yaginuma, H., Shiga, T., Homma, S., Ishihara, R., and Oppenheim, R. W. (1990). Identification of early developing axon projections from spinal interneurons in the chick embryo with a neuron specific beta-tubulin antibody: Evidence for a new "pioneer" pathway in the spinal cord. *Development* **108,** 705–716.

Yamada, T., Placzek, M., Tanaka, H., Dodd, J., and Jessel, T. M. (1991). Control of cell pattern in the developing nervous system: Plarizing activity of the floor plate and notochord. *Cell* **64,** 635–647.